LISE++

version 7.6

RF separator

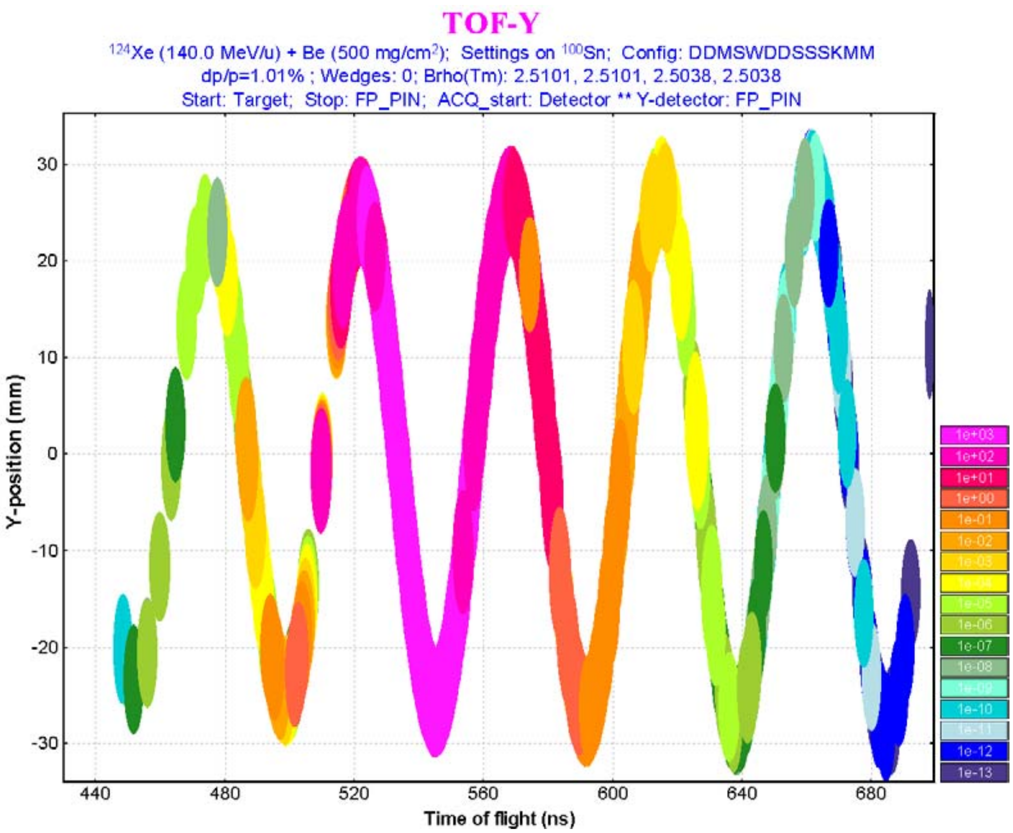

www.nscl.msu.edu/lise
dnr080.jinr.ru/lise

East Lansing
August-2006

Contents:

1. RF separator

The new optical block “RF separator” has been implemented in the LISE++ code. The main aim of RF deflector system is to increase the fraction of proton-rich nuclei of interest in RI beams. Development of this block in the code was based on the calculation results done for the RF separator system proposal at NSCL [RFS05]. A fragment of this proposal was used in the next chapter to introduce in RF Separation System substance. An RF deflector system was already constructed and installed at the RIKEN Projectile-Fragment Separator (RIPS), and comparisons between RIKEN experimental results and LISE++ calculations are presented in this manual.

1.1. RF Separation System (RFSS) proposal at NSCL

The proposed RF Separation System (RFSS) at NSCL consists of three Superconducting quardrupole doublets to provide transverse focusing for the secondary beams from A1900 Fragment Separator, three vertical steering dipole magnets to keep the desired secondary beam component on axis, a RF Kicker (RFK) to provide vertical beam separations for different secondary beam species due to their different Time of Flight (TOF), and a slit system in the 2nd beam diagnostics box for final beam selection. Fig.1 shows the layout of the proposed RFSS in the experimental area of NSCL.

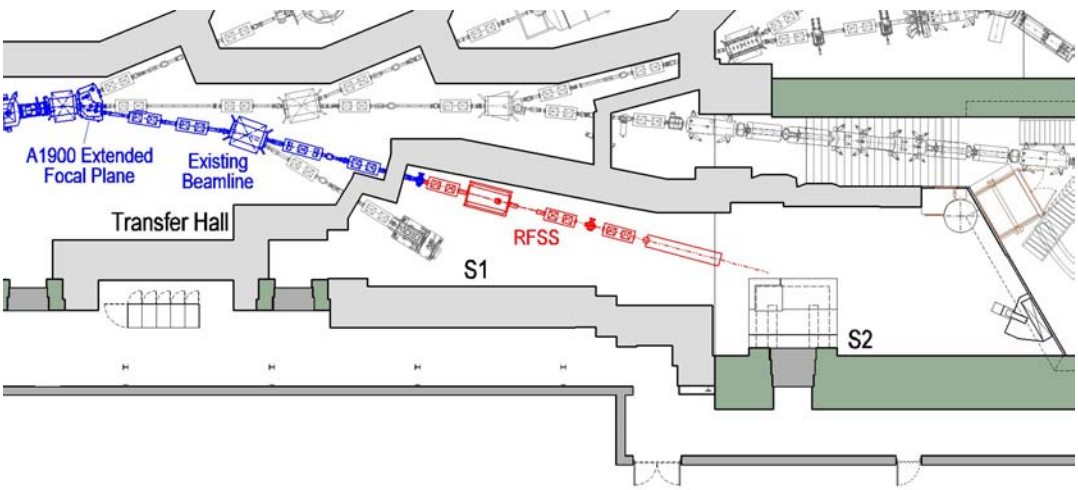

Fig.1. *The layout of the proposed RFSS at NSCL.*

As show in Fig.1, the RFSS will be occupying the S1 Experimental Hall at NSCL. The existing beam line will transport the secondary beams from the A1900 Extend Focal Plane (XFP) to the 1st Beam Diagnostics Box with desired transverse beam conditions. A quadrupole triplet and a doublet located between the last dipole of the beam line and the wall of the S1 Experimental Hall will be used for the transverse phase space matching.

Fig.2 shows the schematic diagram of the RFSS. The 1st quadrupole doublet will provide initial transverse focusing for the secondary beam from the existing beam line. The acceptance of the existing beam line is assumed to be < 80π mm-mrad. The RFK will provide vertical beam separations for different secondary beam species due to their different Time of Flight (TOF). Three vertical steering dipole magnets in front of and after the RFK will be used to cancel the RFK’s effect on the beam centroid of the desired ion and keep it on the beam axis. The 2nd quadrupole doublet will achieve a desired beam transverse phase spaces at the slit inside the 2nd beam diagnostics pot. After the desired secondary beam is selected, the 3rd quadrupole doublet will provide the transverse focusing to the detector target. The three-quadrupole-doublets focusing will also provide sufficient transverse focusing and matching flexibilities in this beam line for other experiments at NSCL, which do not require RF Kicker in the future.

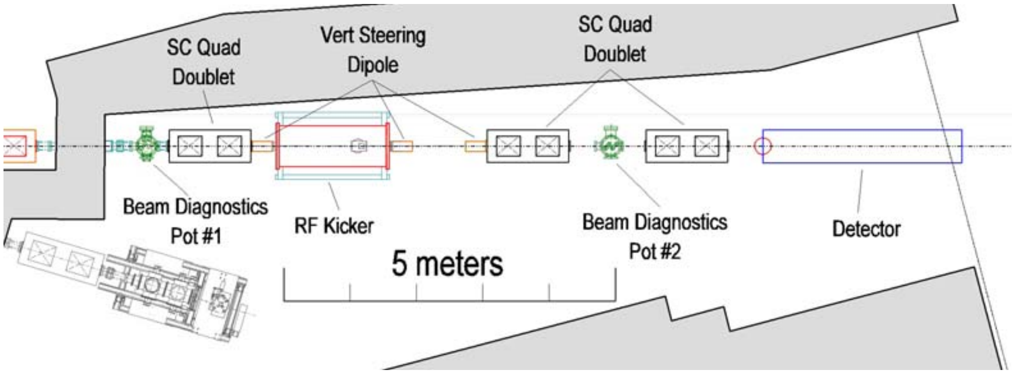

Fig.2. Schematic diagram of the RFSS.

The RF Kicker is the most important components in the proposed RFSS, and provides vertical beam separations for different secondary beam species due to their different Time of Flight. The RF Kicker will be operated at the K1200 Superconducting Cyclotron frequency in the range of 23 ± 5 MHz, depending on the primary beam energy required for the experiment. The proposed RF kicker design uses a pair of parallel plates with length of 1.5 m, width of 10 cm and gap of 5 cm. With such a design, secondary beams with transverse emittances of about 80π mm-mrad can be accommodated and the electric field uniformity within the beam region is about ± 2%. The voltage applied on these plates will be sinusoidal with a peak voltage of 100 kV, resulting in a peak electric field of 20 kV/cm.

1.2. Construction of the "RF separator" block in LISE

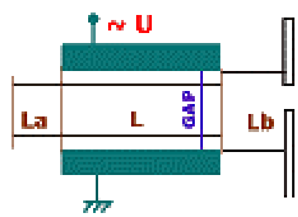

Fig.3. Scheme of the RFSS.

The RF separator system can be separated on three parts (see Fig.3):

1. The first part (by a length *La*) provides a parallel beam from the Beam diagnostics #1 (see Fig.2) up to the RF kicker block.

2. The second part (by a length *L*) is the RF kicker itself.

3. The third part (by a length *Lb*) focuses a beam in the Beam diagnostics #2.

The RF separator block in LISE is based on the "optical dispersive block" standard class which the charge state (Z-Q) property assigns for block tuning. The LISE code assumes the RF separator block consisting from two blocks:

1. The Drift block which corresponds to the first part of the RFSS with the same length La. The important task of this unit to form a beam from a point in parallel using an optical matrix which we explicitly shall stay later.

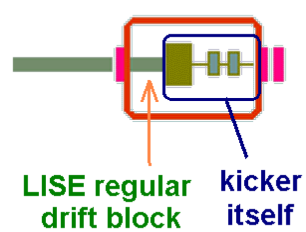

Fig.4. The RFSS in LISE.

2. The LISE RF separator block joins the second and third parts of the RFSS (see Fig.4). The local optic matrix of block reshapes a beam parallel to point. Dispersion parameters are equal to zero. Ion deflection by electrodes in the code implements irrespective of optical matrixes with a zero dispersion based on the final spatial coordinate shift. Calculation principles of this shift are given in chapter "1.2.2. Deflection by RF kicker".

1.2.1. Optics

According to the NSCL RFSS proposal[♣] the beam ellipses are rotated (matrix elements R12≠0 and R34≠0) before and behind the first part of RFSS ("*La*" block). But LISE++ does not support rotated ellipses suggesting both correlations R12 and R34 equal to zero. In order to LISE optics corresponds to NSCL-RFSS calculations it is necessary to create two optical matrices for LISE:

1. The first matrix (assigned to the drift block before the RF kicker) transforms a beam vector after the A1900 separator to parallel with the same ellipses parameters (x,x`,y,y`) as were calculated by NSCL-RFSS;
2. The second matrix (assigned to the RF kicker block) transforms a beam vector after the drift block to an ellipse analogous to NSCL-RFSS calculations.

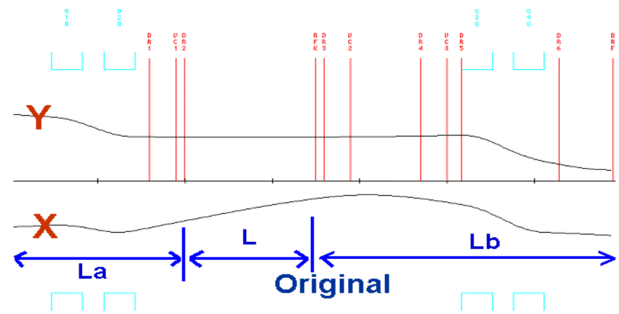

***Fig.5**. Envelope calculated by the TRANSPORT code corresponding to NSCL-RFSS values. R12 and R34 correlation parameters of the input beam are equal to -0.548 and -0.842 correspondingly.*

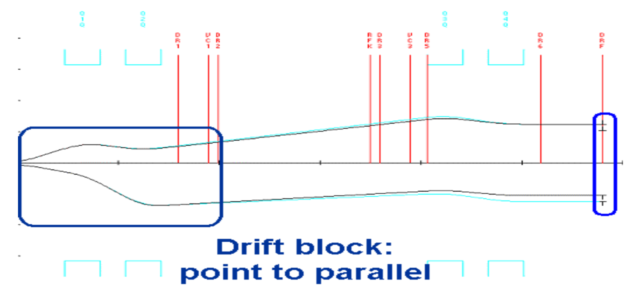

***Fig.6**. Envelope corresponding to "point to parallel" transformation. R12 and R34 correlation parameters of the input beam after the A1900 fragment-separator are equal to zero. Calculations were done to get the optical matrix of the drift block before the RF separator block in LISE.*

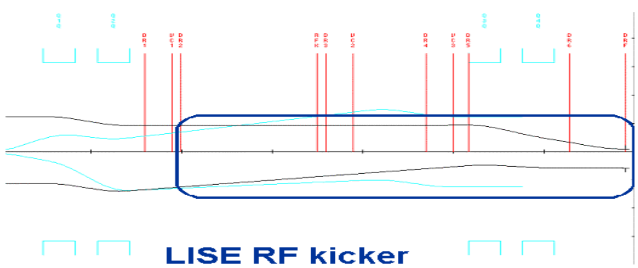

***Fig.7**. RK separator block envelope calculated by the TRANSPORT code. Input beam parameters were taken from the envelope shown in Fig.6.*

Global matrix

							Beam
1.656	0.0001	0	0	0	0.0011	[mm]	1.656
-2.3756	0.6038	0	0	0	0.0003	[mrad]	12.308
0	0	1.1464	0.0002	0	0	[mm]	1.146
0	0	9.0038	0.8735	0	0.0001	[mrad]	19.653
0	0	0	0	1	0	[mm]	0
0	0	0	0	0	1	[%]	0.07
/[mm]	/[mrad]	/[mm]	/[mrad]	/[mm]	/[%]		

Det = 0.99993

***Fig.8**. The "Global" matrix and the beam vector after the A1900 fragment-separator usable in LISE.*

Block matrix

1. X	-0.5652	1.708	0	0	0	0
2. T	-0.5843	-0.0036	0	0	0	0
3. Y	0	0	-7.5327	1.157	0	0
4. F	0	0	-0.6996	-0.0253	0	0
5. L	0	0	0	0	1	0
6. D	0	0	0	0	0	1
	/[mm]	/[mrad]	/[mm]	/[mrad]	/[mm]	/[%]

Det = 1.00003

Global matrix

							Beam
-4.9935	1.0313	0	0	0	-0.0002	[mm]	21.221
-0.9591	-0.0022	0	0	0	-0.0006	[mrad]	0.96
0	0	1.7819	1.0094	0	0	[mm]	20.266
0	0	-1.0298	-0.0222	0	0	[mrad]	1.122
0	0	0	0	1	0	[mm]	0
0	0	0	0	0	1	[%]	0.07
/[mm]	/[mrad]	/[mm]	/[mrad]	/[mm]	/[%]		

Det = 0.99996

***Fig.9**. The local matrix of the drift block (La) before the RF separator block, the global matrix and the beam vector after the drift block.*

Block matrix

1. X	0.4072	7.407	0	0	0	0
2. T	-0.0445	1.6461	0	0	0	0
3. Y	0	0	-0.0162	2.284	0	0
4. F	0	0	-0.4227	-2.1294	0	0
5. L	0	0	0	0	1	0
6. D	0	0	0	0	0	1
	/[mm]	/[mrad]	/[mm]	/[mrad]	/[mm]	/[%]

Det = 0.99985

Global matrix

							Beam
-9.1371	0.4036	0	0	0	-0.0047	[mm]	12.192
-1.3565	-0.0495	0	0	0	-0.001	[mrad]	1.68
0	0	-2.381	-0.0671	0	0	[mm]	2.733
0	0	1.4397	-0.3793	0	0	[mrad]	7.722
0	0	0	0	1	0	[mm]	0
0	0	0	0	0	1	[%]	0.07
/[mm]	/[mrad]	/[mm]	/[mrad]	/[mm]	/[%]		

Det = 0.99981

***Fig.10**. The local matrix of the RF separator, the global matrix and the beam vector after the RF separator.*

♣ we use for citations in future "NSCL-RFSS".

Fig.5 shows the beam envelope for the NSCL RF separator system. Fig.6 and Fig.7 show the beam envelopes to obtain LISE matrices for the drift block and the RF separator assuming input beam correlation parameters (R12 and R34) equal to zero.

Fig.8, Fig.9, and Fig.10 show global matrices and beam vectors after the A1900 fragment-separator, the drift block before the RF separator, and the RF separator accordingly. Fig.9 and Fig.10 show as well as local block matrices.

The entrance of RFSS is about 52 m away from the A1900 production target. We put in the "A1900_Kicker.lcn" configuration file a drift block (length 15 m) with an unitary block optic matrix to fill up a missing length after the A1900 fragment-separator (see Fig.11).

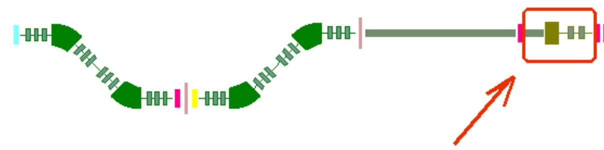

Fig.11. *The set-up scheme corresponding to the "A1900_Kicker.lcn" configuration file provided by the LISE installation package.*

Fig.12 shows the envelope through the A1900 & RF separator system for ^{100}Sn fragments produced in the ^{124}Xe (140MeV/u) + Be(447mg/cm^2) reaction.

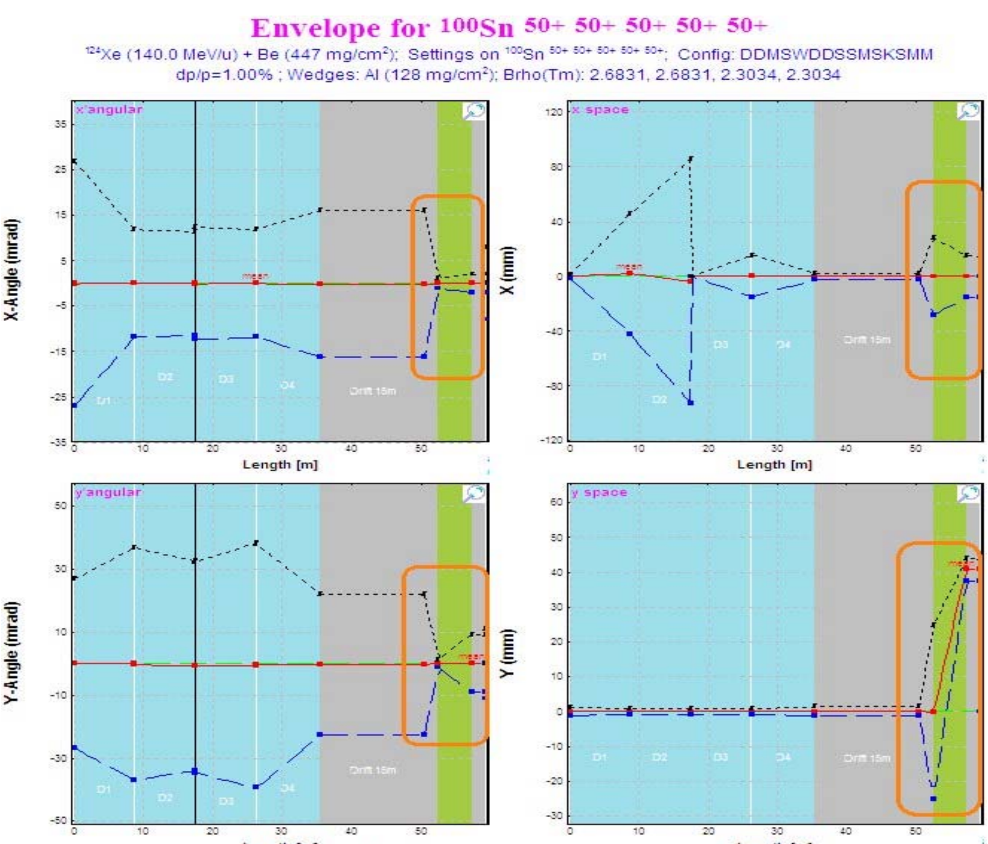

Fig.12. *Envelope through the A1900 & RFkicker system for ^{100}Sn fragments produced in the ^{124}Xe (140MeV/u) + Be(447mg/cm^2) reaction. The spectrometer is tuned on the ^{100}Sn fragment.*

Rounded rectangles show the RF separation system which consist of the drift block and the RF kicker block.

The vertical spatial envelope demonstrates deflection of ^{100}Sn fragments by the RF separator tuned on the maximal deflection value (see Fig.17).

Fig.13 shows the NSCL-RFSS beam envelope calculated for the beam diagnostics pot #1 (see Fig.2) and the LISE beam envelope calculated for the point between the drift block (*La*) and the RF separator block. The vertical position of NSCL_RFSS beam envelope is a little bit larger than one calculated by LISE because we compare envelopes in different places. As you can see from Fig.5 the vertical position of NSCL_RFSS beam envelope decreases at the point before the RF kicker comparing with the initial position.

Fig.14 shows NSCL-RFSS and LISE beam envelopes calculated at the slit selection after RFSS.

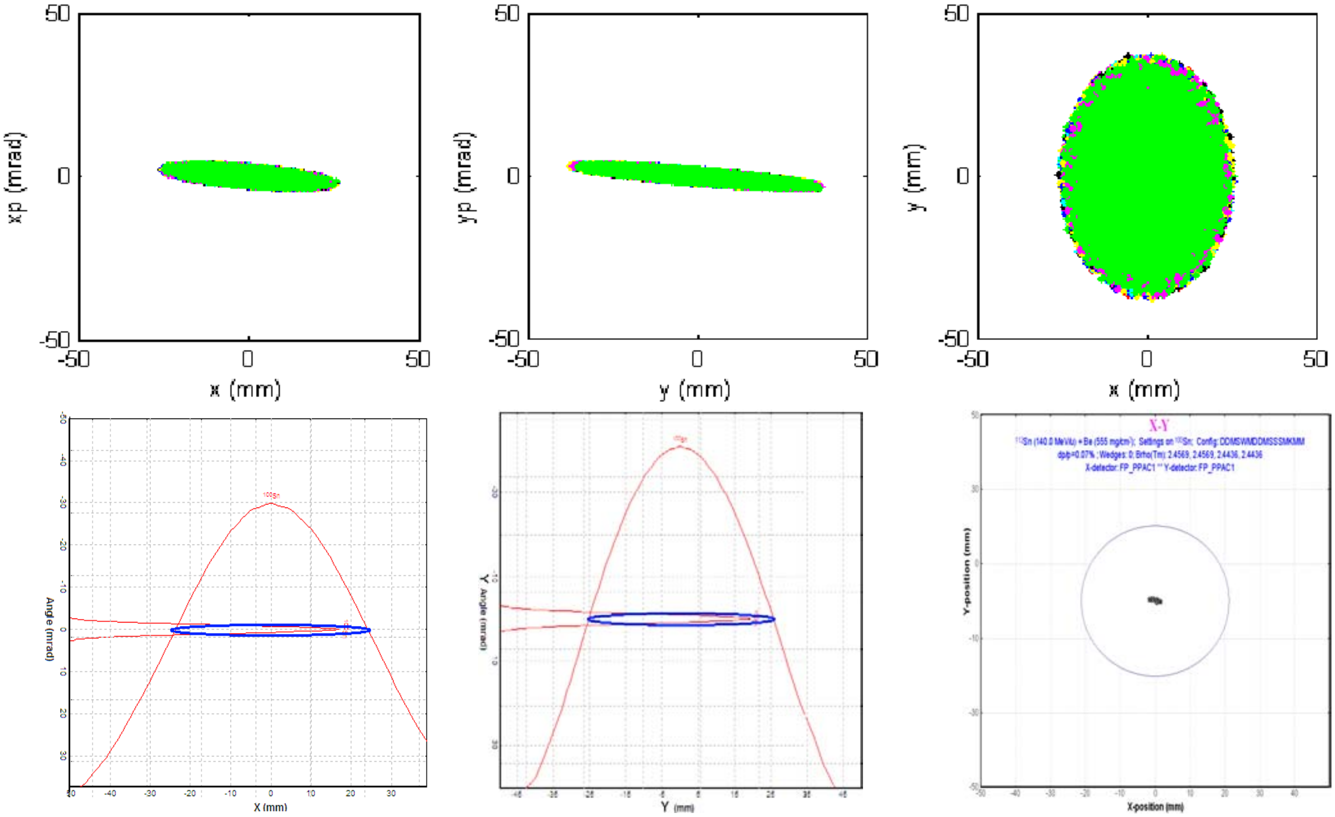

Fig.13. *NSCL-RFSS beam envelope (top plots) calculated for the beam diagnostics pot #1 (see Fig.2) and the LISE beam envelope (bottom plots) calculated for the point between the drift block (La) and the RF separator block. X-θ plane ellipses are shown in left plots, and Y-ϕ and X-Y plane ellipses accordingly on middle and right plots.*

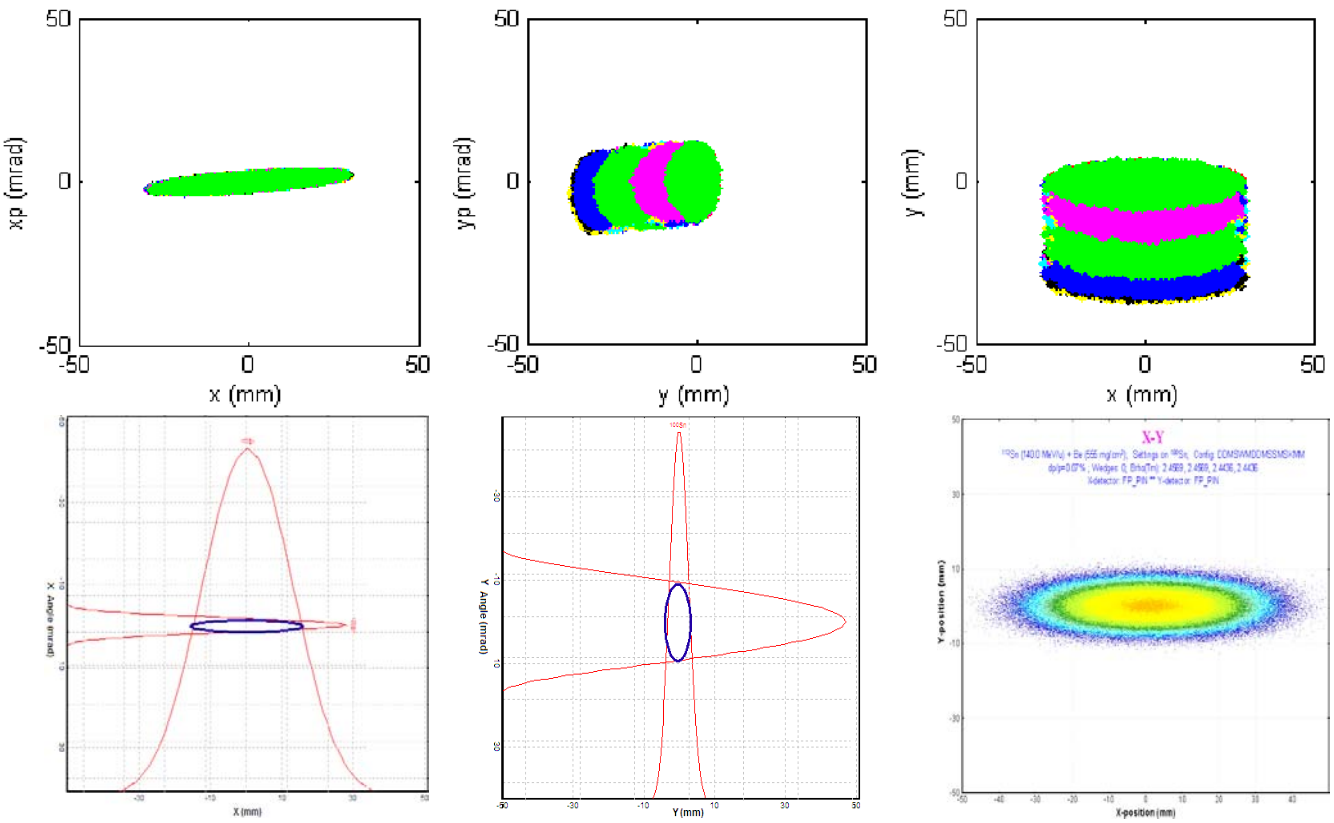

Fig.14. *NSCL-RFSS and LISE beam envelopes calculated at the slit selection after RFSS.*

1.2.2. Deflection by RF kicker

A vertically arranged parallel-electrode of the RF separator is set along the beam line, and high voltage of sinusoidal form is applied to the electrode in the direction perpendicular to the beam axis. The sinusoidal voltage V is written as $V = V_0 \sin(\omega t + \varphi)$, it should be noted that the oscillation phase φ is defined as the phase of the sinusoidal voltage when the particle arrives at the upstream **start** of the electrode. Let's introduce a value a_0 for the following calculations. The physical meaning of this value is maximum acceleration which can be reached by an ion under the influence of electric filed:

$$a_0 = \frac{V_0\, q}{d\, m}, \qquad /1/$$

where q and m are the electric charge and mass of the ion, d is the gap size of electrodes. Then the ion vertical velocity between electrodes at the moment t can be written as,

$$\upsilon_y(t) = \upsilon_{y0} + \int_0^t a_0 \sin(\omega t + \varphi)\, dt\,. \qquad /2/$$

The vertical position Y of a beam particle between the electrodes can be written in the first order as

$$Y_1(t) = Y_0 + \int_0^t \upsilon_y(t)\, dt + L(t)\cdot Y_0^{'}\,, \qquad /3/$$

where Y_0 and $Y_0^{'}$ are the initial position and angle of the particle, $L(t)$ is the path passed by the ion between the electrodes which is equal to ($\upsilon_z t$), where υ_z is the beam axis ion velocity.

The vertical position Y_B of the beam particle after RFSS can be written as,

$$Y_B = Y_1(\tau) + L_B \cdot \left(Y_0^{'} + \upsilon_y(\tau)/\upsilon_z\right), \qquad /4/$$

where L_B is the length of third part of RFSS, and τ is the flight time of the ion between electrodes by length L0: $\tau = L_0 / \upsilon_z$.

Suggesting initial input parameters ($Y_0\,, Y_0^{'}, \upsilon_{y0}$) being equal to zero it is possible to get the vertical position just after the electrodes almost the same way at it was received in [Yam04] :

$$Y_1 = \frac{a_0 \tau}{\omega}\cdot\cos(\varphi) + \frac{a_0}{\omega^2}\cdot\left[\sin(\varphi) - \sin(\tau\omega + \varphi)\right]. \qquad /5/$$

1.2.3. RF separator general settings

The RF separator block can be inserted in the spectrometer by regular way using the "Spectrometer designing" dialog (see Fig.15). Designations of the RF separator in the LISE scheme you can see in Fig.11.

Note: Do not forget to insert a drift block with the point-to-parallel matrix before the RF separator block to provide a parallel beam for the RF separator and to keep the total length of blocks because the LISE RF separator block does not contain the first part of RFSS (see Fig.2).

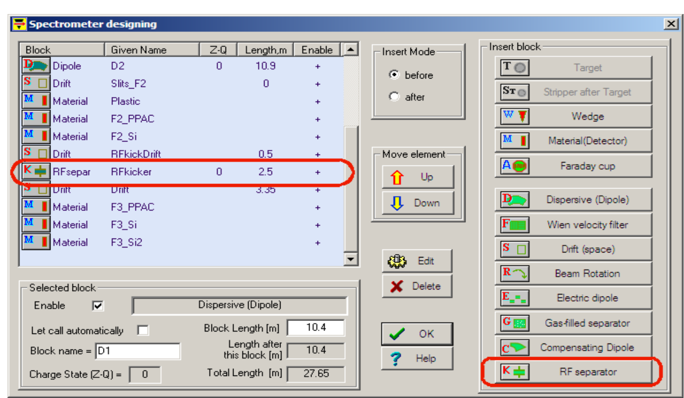

Fig.15. *The "Spectrometer designing" dialog. RF separator buttons are marked by rounded rectangles.*

The RF separator dialog is shown in Fig.16. Using this dialog the user defines voltage applied to RF separator electrodes, the gap between electrodes, block geometry, the phase shift value and a method how to tune a block. The dialog shows for the setting fragment calculated values of the time of flight up to the block, average energy, corresponded phase and position in selection slits after the block as well as their variations corresponded to a momentum acceptance of the spectrometer. Two utilities have been implemented in the dialog in order to see the beam profile for different phase shifts and to make block settings optimization on purity and intensity (see corresponding buttons in Fig.16).

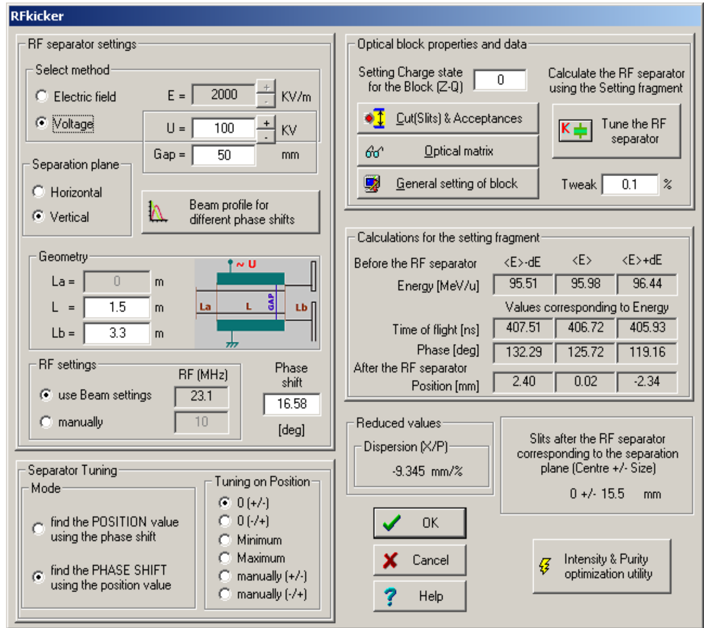

Fig.16. *The "RF separator" dialog.*

Fig.17 shows beam profile distributions as a function of phase shift for the setting fragment and its neighbors as well as position variations from a fragment energy spread and an initial angle.

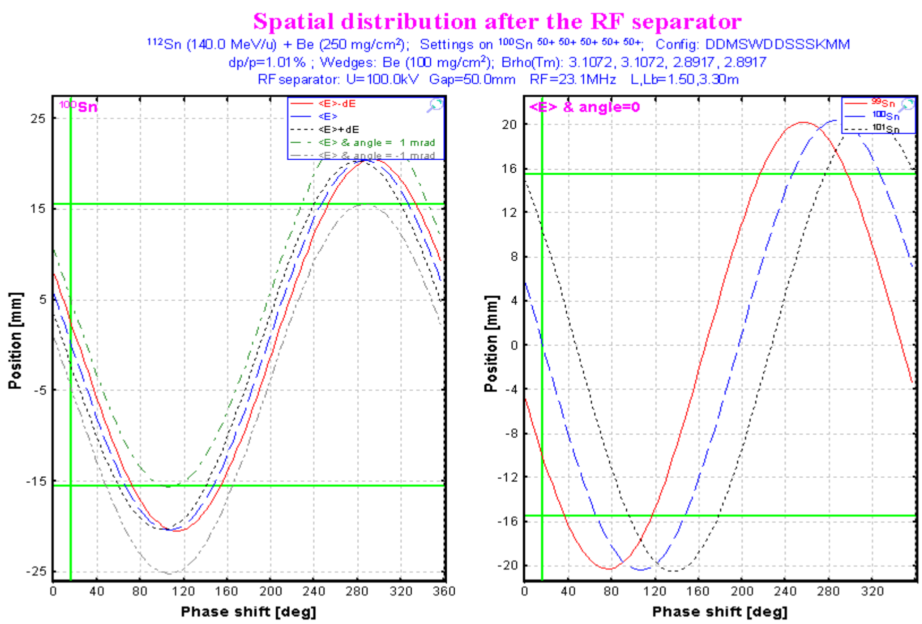

__Fig.17__. Beam profile distributions after the RF separator as a function of phase shift.

Left plot shows position variations as function of energy spread (from a momentum acceptance) and initial angle values.

Right plot shows positions of isotopes neighboring to the setting fragment.

Horizontal green lines show selection slit positions after the RF separator, and a vertical line shows a value currently set in the "RF separator" dialog.

The reduced dispersion value (X/P) shown in the dialog corresponds to a centre of the fragment energy distribution and is used only for Monte Carlo 2D-plots drawing. Actually momentum dispersion due to deflection by electrodes if function of selection slits position. Dispersion maximum value reaches at Y=0 whereas the reduced dispersion is equal to zero at maximal and minimal positions.

1.2.4. RF separator tuning

RF separator is the especial block if to compare to other dispersive blocks in which one selection is based on change of electrical or magnetic fields. In the RF separator case a voltage value determines an amplitude of a sine wave, but the selection is made by choice of the phase shift and slits position.

RF separator block tuning at the choice of the user (see the “Separator Tuning” frame in Fig.16) implies or the slits position setting for the fixed phase shift or to the contrary tuning of the phase shift for the fixed slits position.

Phase shift search can be carried out for six different cases of slits position. The program can find an phase shift which one corresponds to maximum or minimum positions (where the dispersion is equal to zero point), a position equal zero, or for position set manually by the user. In last two cases there are two versions of search. When the dispersion is positive (the curve goes from negative values to positive values or “-/+”) and when a dispersion is negative (sign “+/-“).

There are no the buttons “Calculate block values from neighbor optical blocks” as it was done for other dispersive optical blocks in the code because the code tunes this block from the target to calculate time of flight. As well as the button “Calculate other blocks” is absent in this dialog because it is impossible to tune other blocks using RF separator settings (phase shift and slits position) as distinct from other dispersive block.

1.2.5. The “Slits” class modification

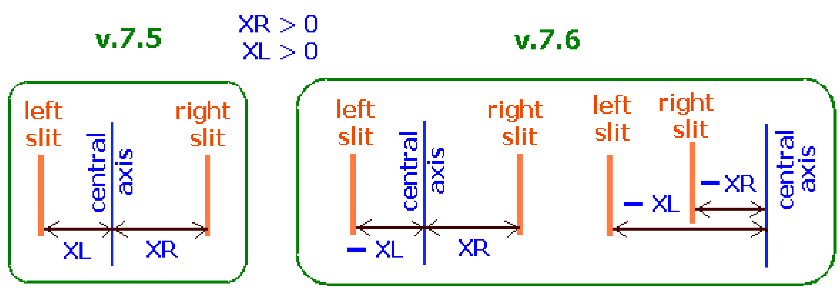

Fig.18. *Layout shows difference in definition of slits between version 7.5 and 7.6.*

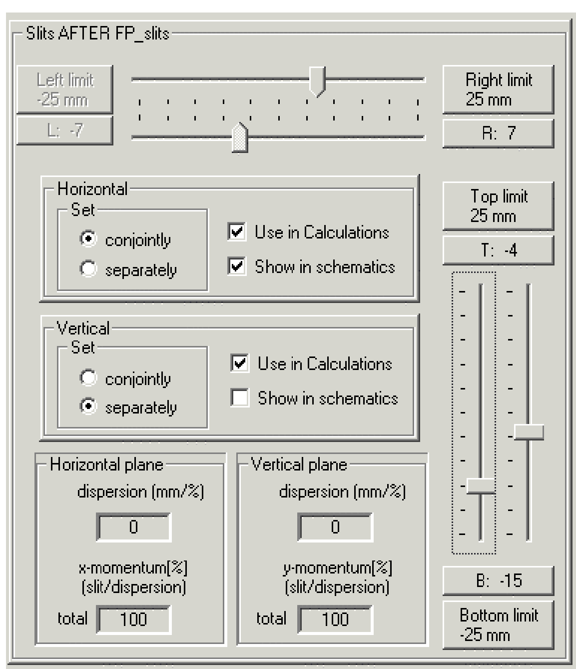

Fig.19. *Fragment of the Slits dialog (v.7.6).*

1.3. Selection by RF kicker

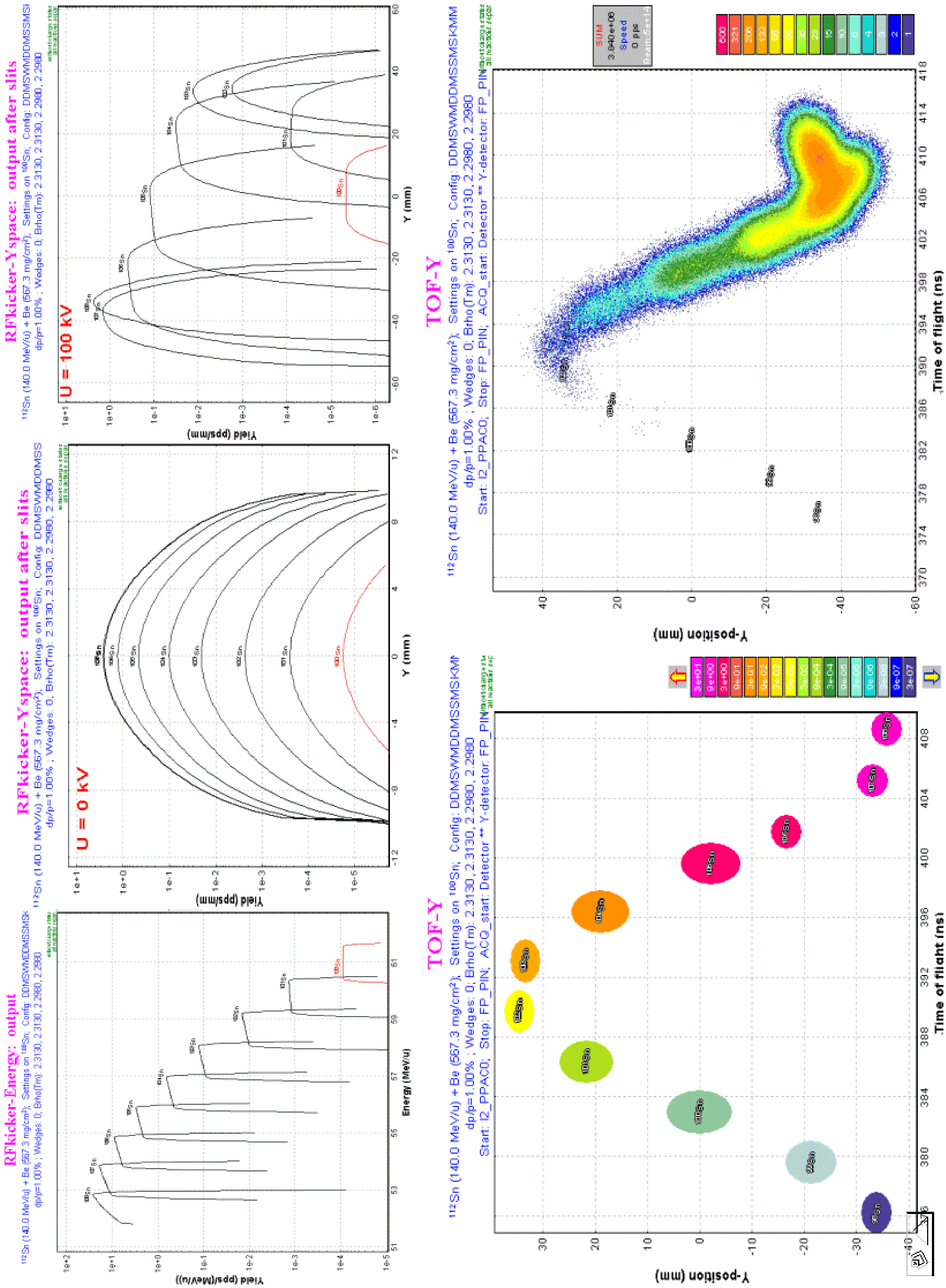

1.4. Acceptance

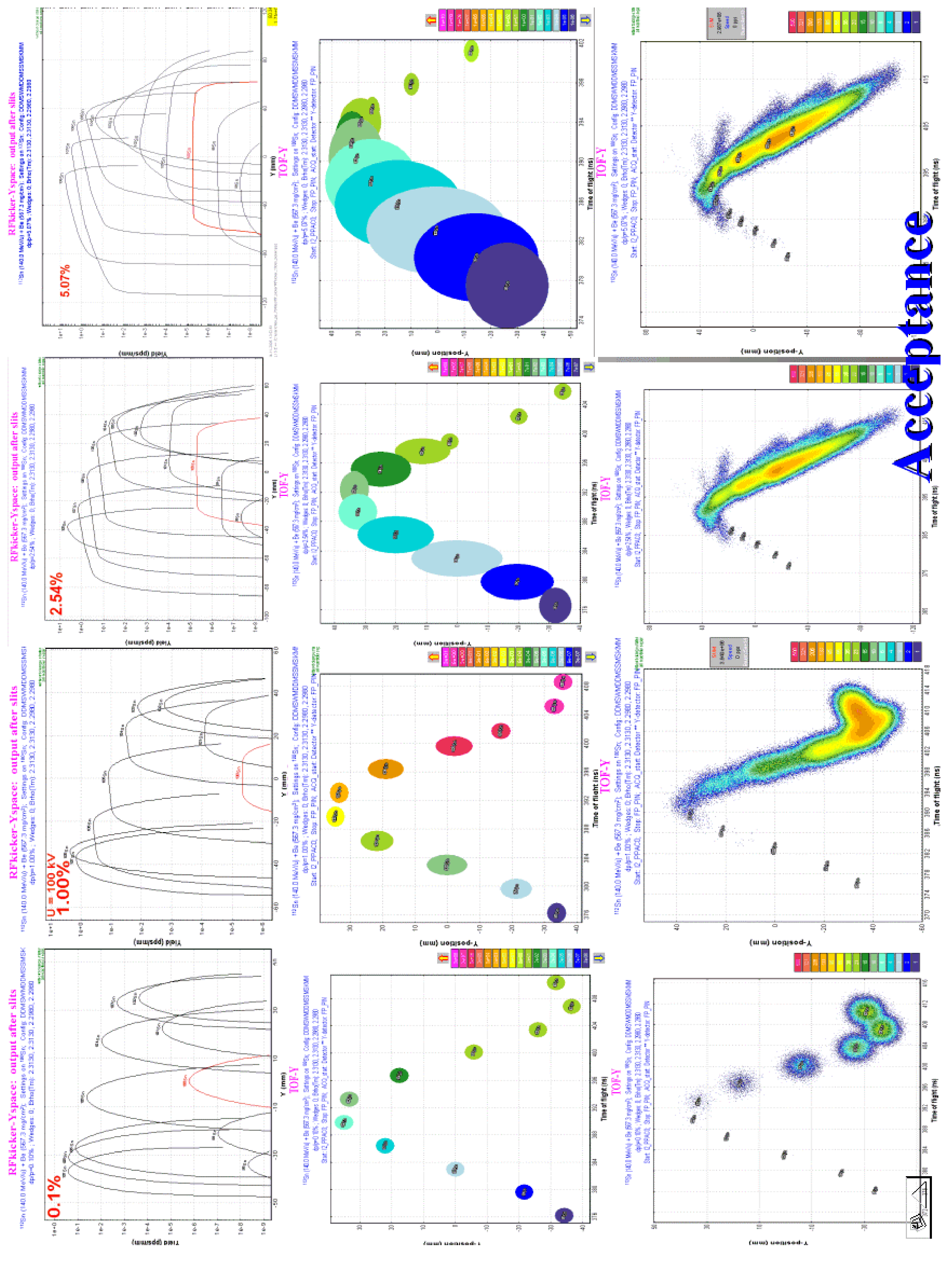

1.5. Comparison with experimental data and other simulation results

1.5.1. RF deflector system in NSCL/MSU

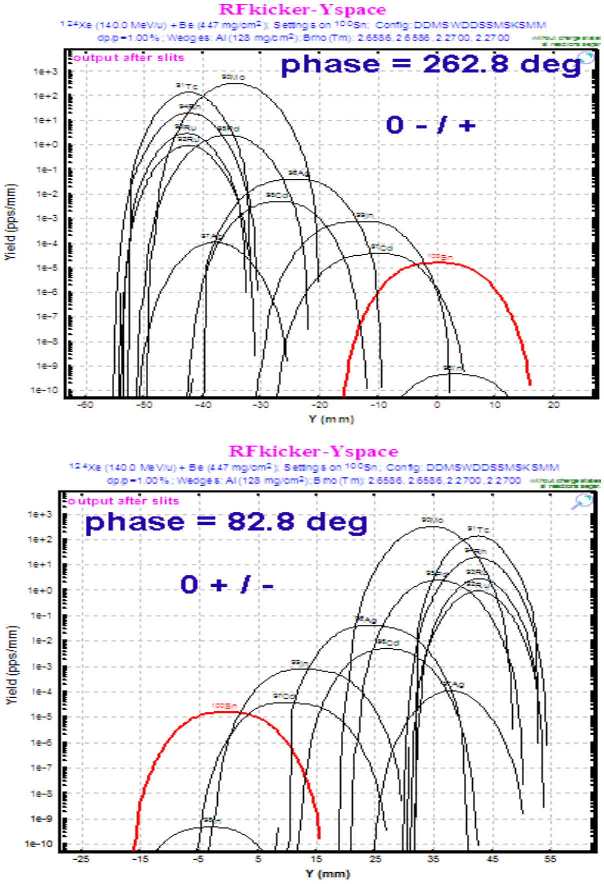

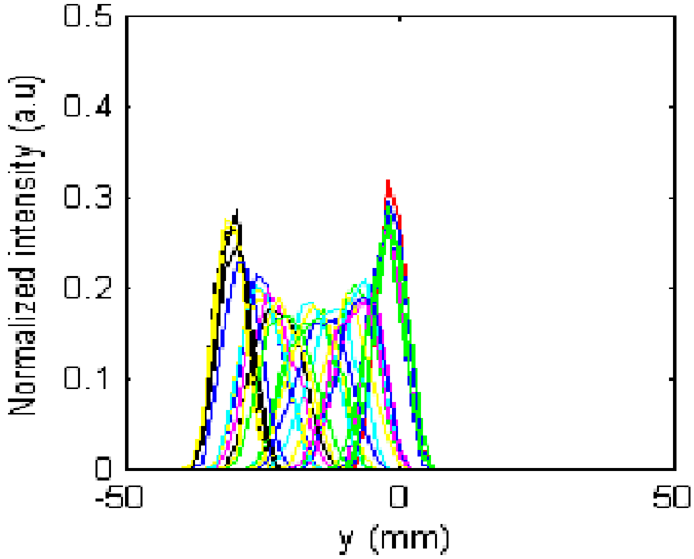

Fig.20. *NSCL RF kicker separation. Left plots demonstrate LISE calculations and the right plot shows the NSCL proposal calculation.*

1.5.2. RF deflector system in RIKEN

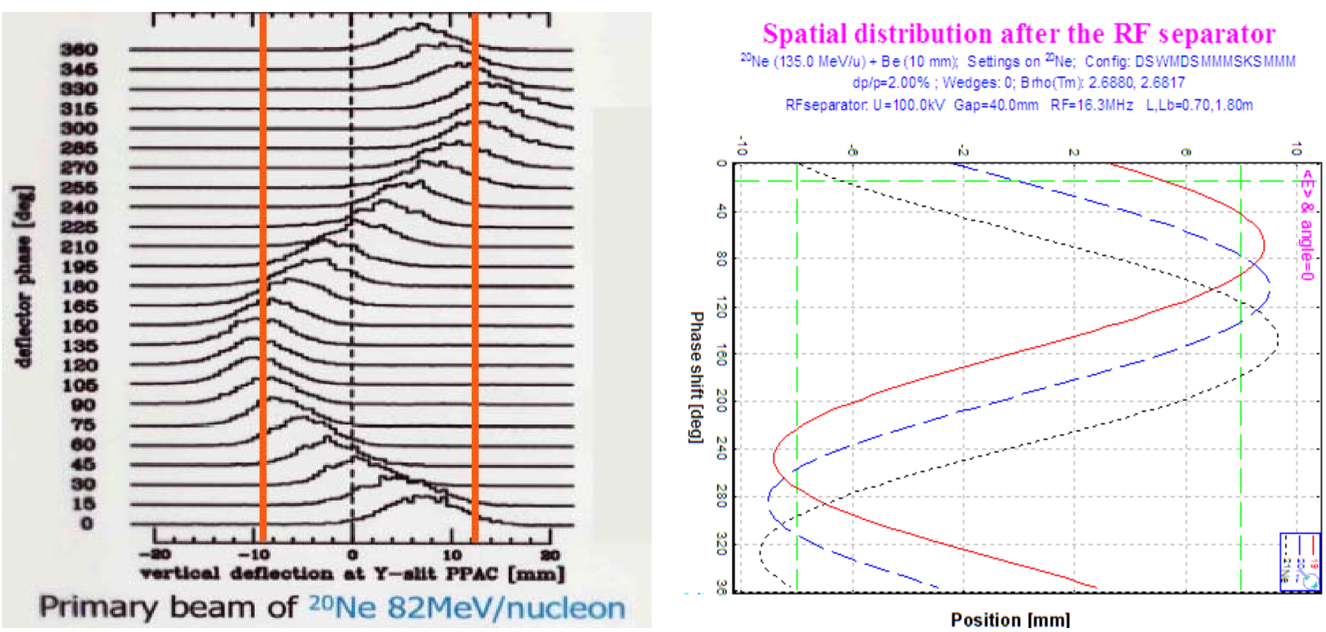

Fig.21. *RIKEN RF kicker separation. The Left plot demonstrate RIKEN experimental data [Yam04] and the right plot shows LISE calculations*

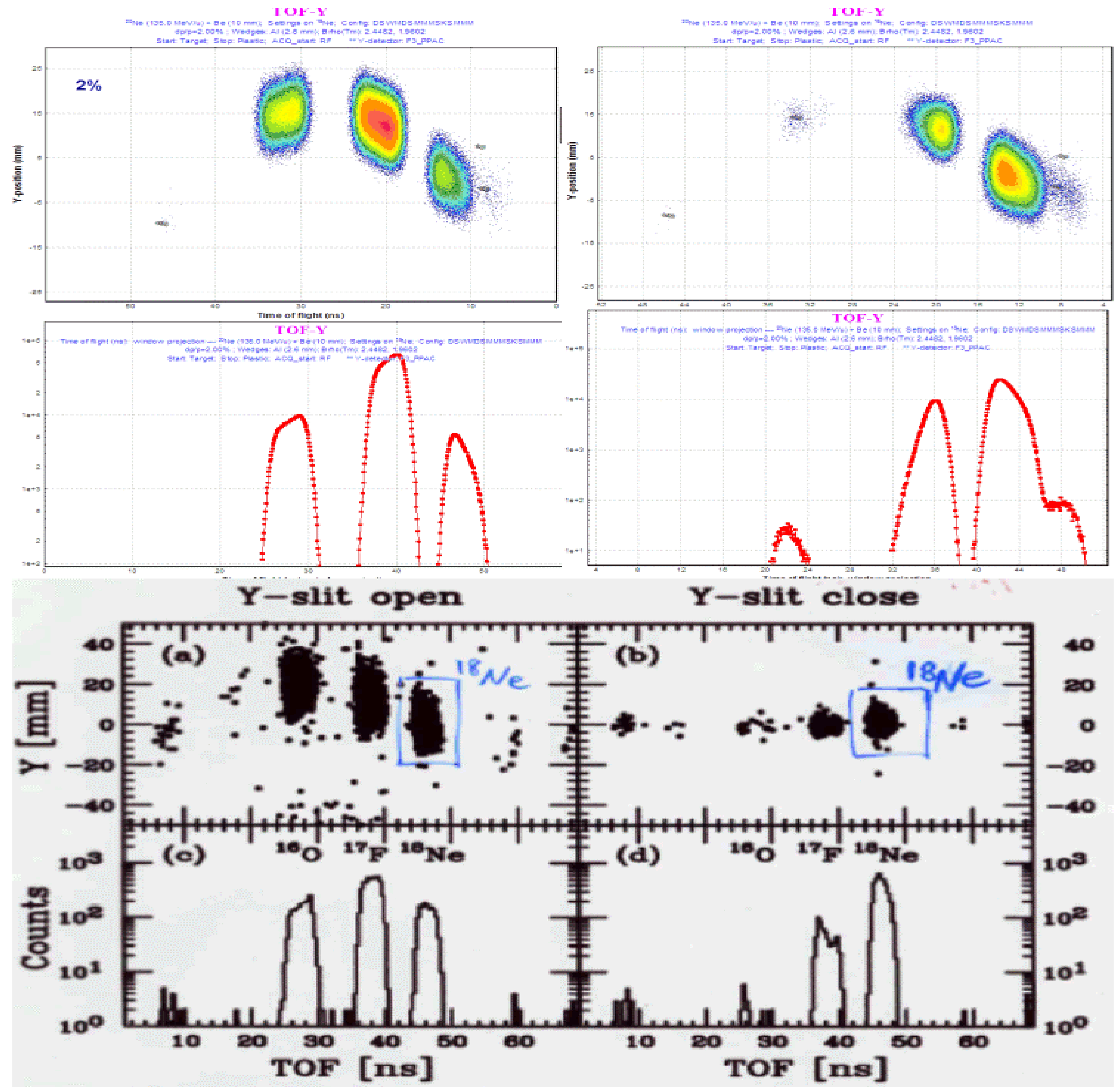

***Fig.22**. RIKEN RF kicker separation. Bottom plots demonstrate RIKEN experimental data [Yam04] and top plots show LISE calculations.*

1.5.2.1. Intensity and purity optimization utility

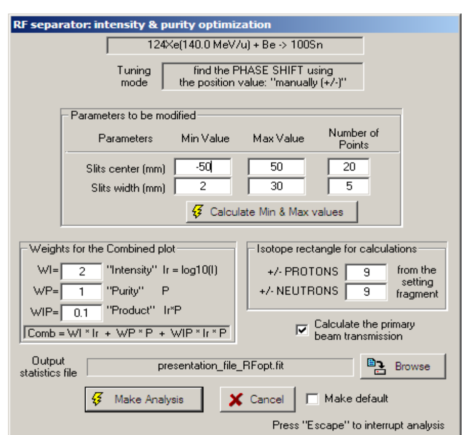

Fig.23. The RF kicker optimization dialog.

Optimization (slits position)

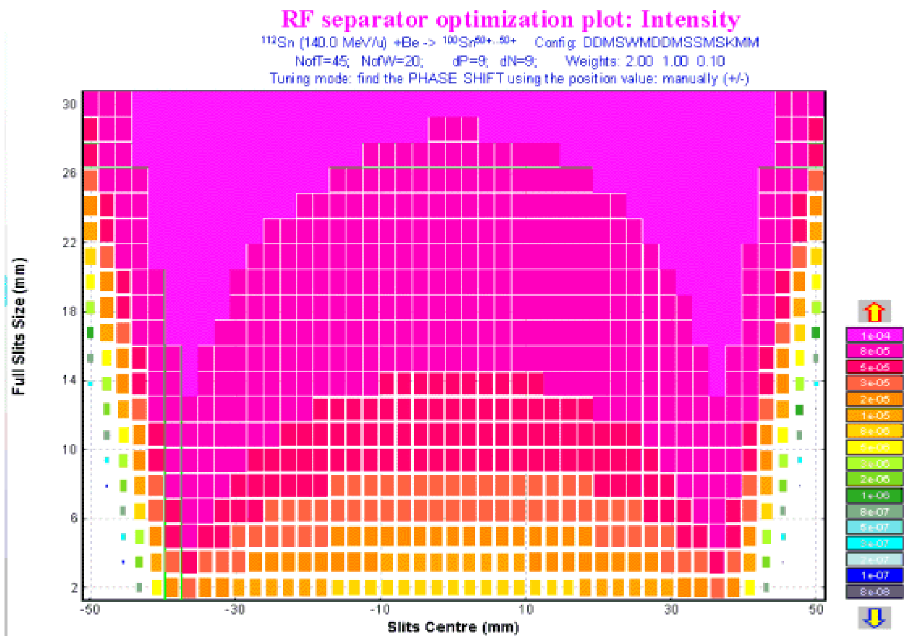

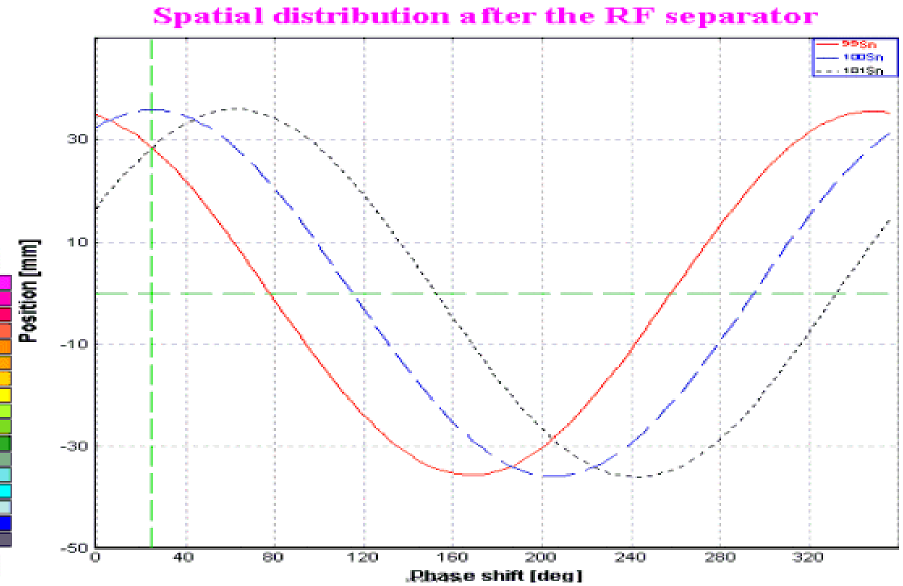

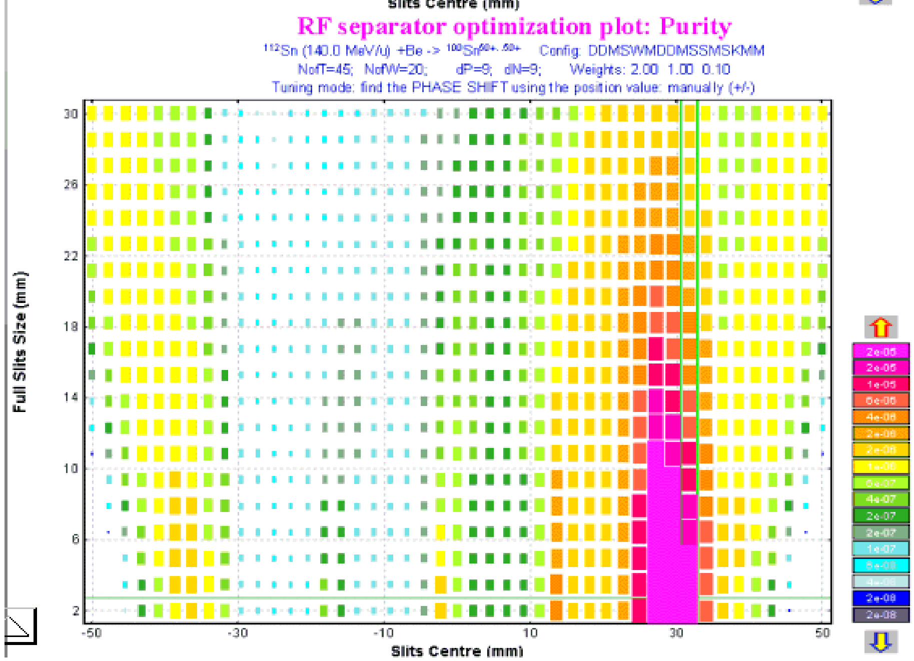

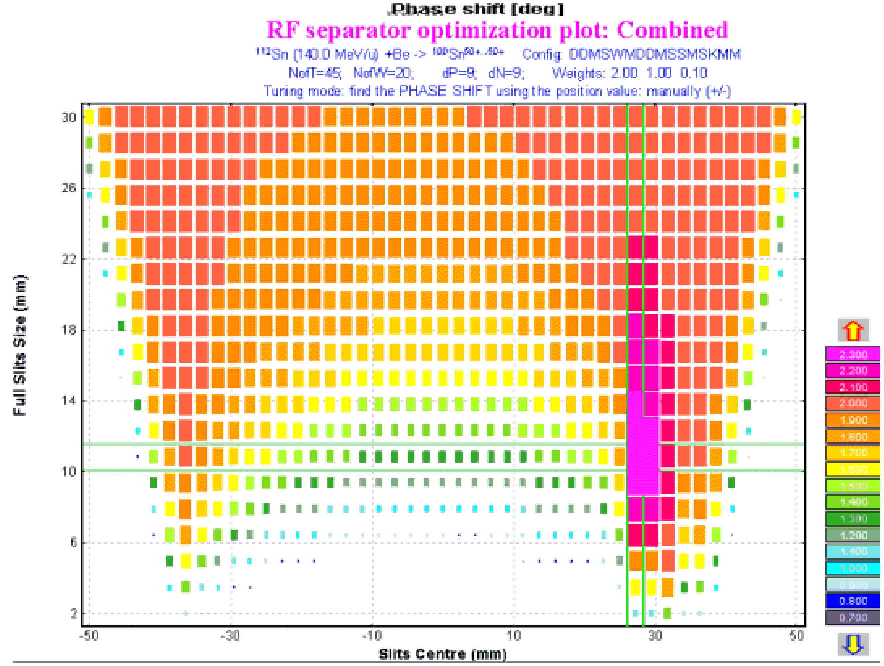

Optimization (phase)

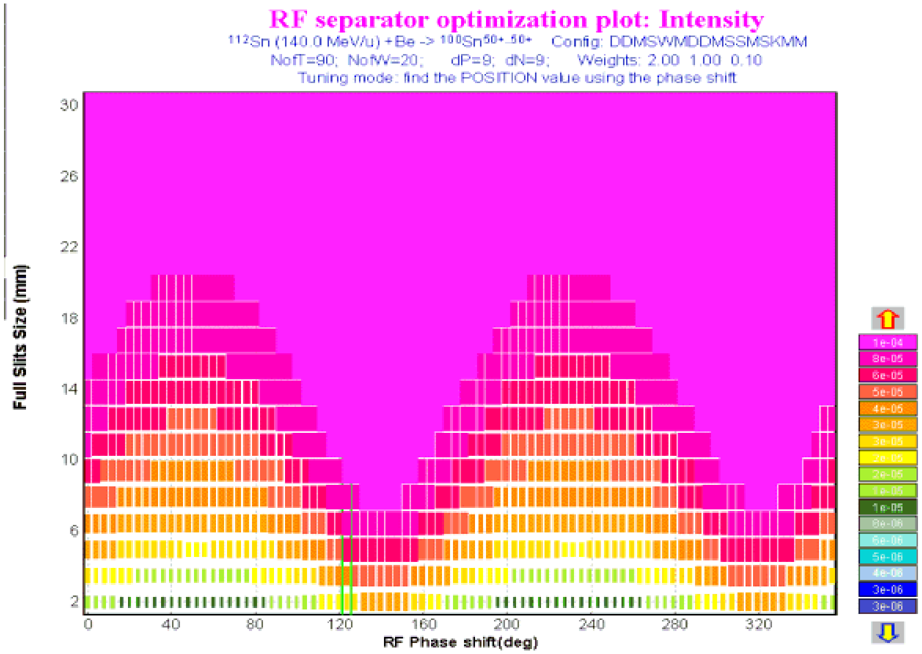

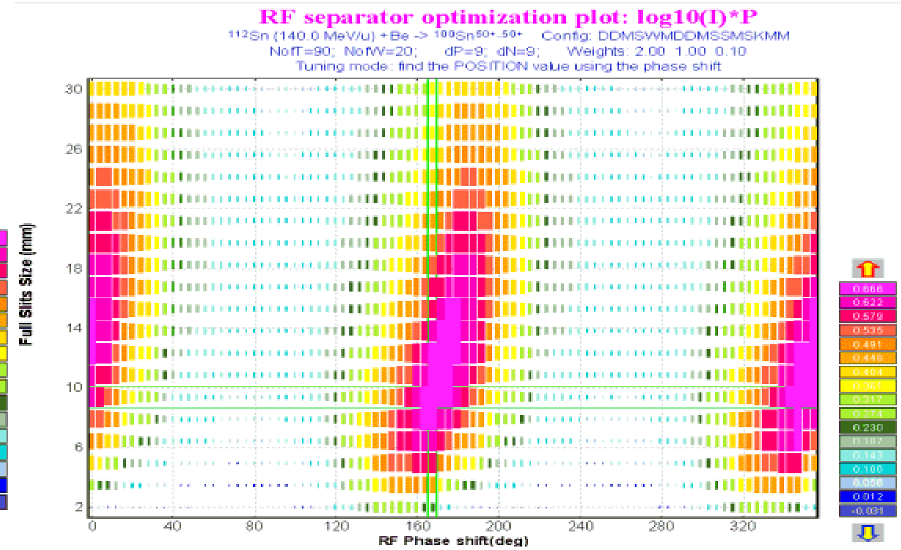

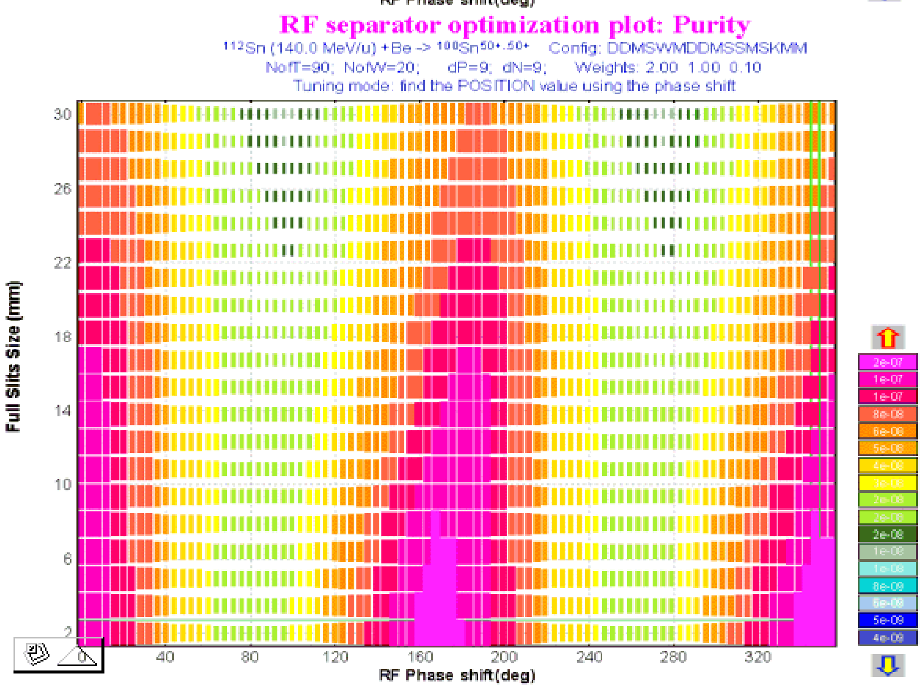

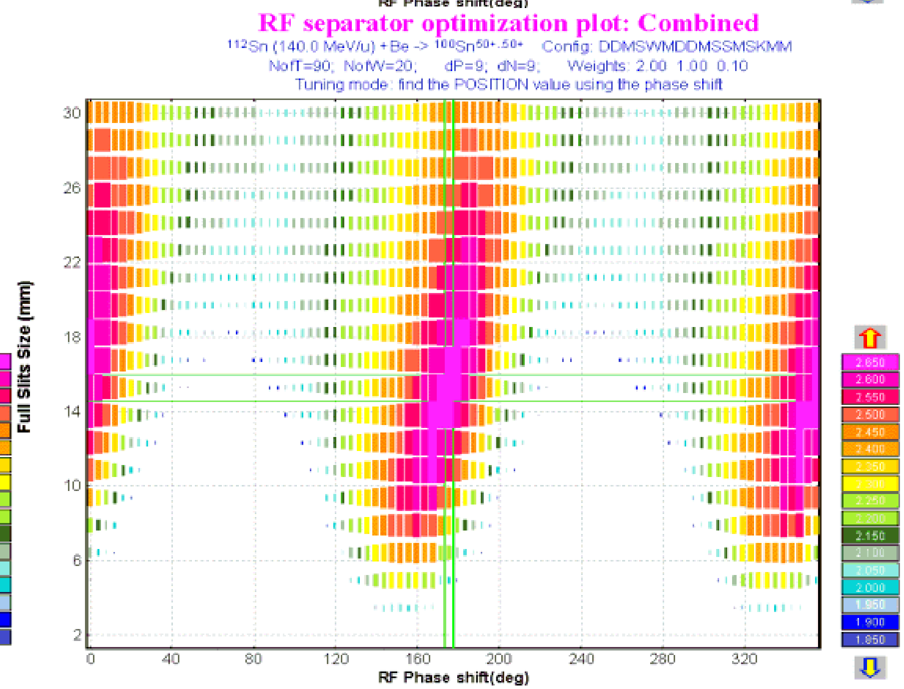

1.6. RF kicker productivity at NSCL

1.6.1. Optimization (target & wedge) to produce ^{100}Sn (60MeV/u)

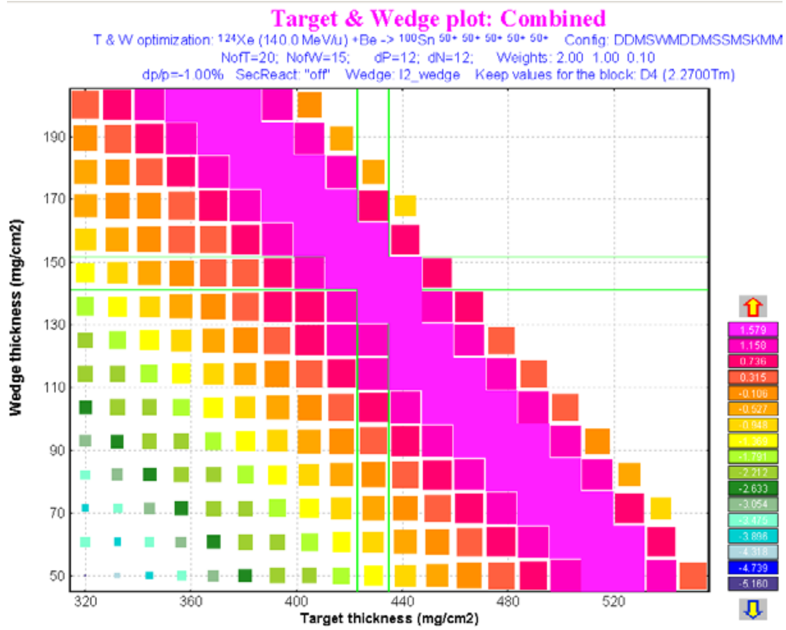

1.6.2. Purification for ^{100}Sn(60MeV/u) without charge states

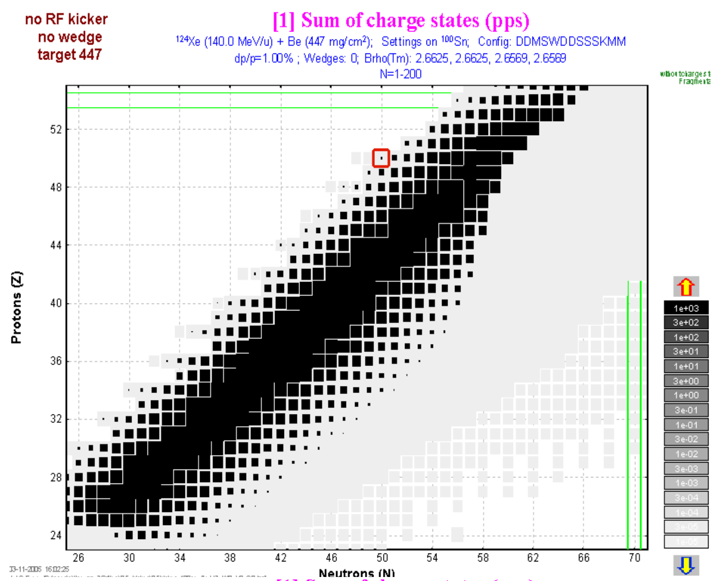

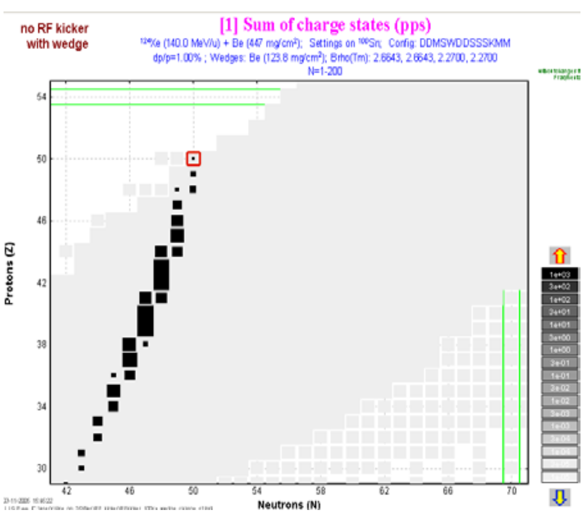

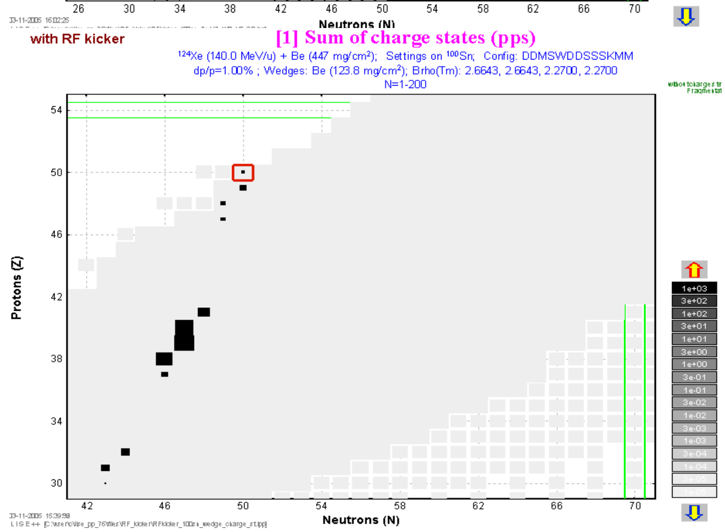

1.6.3. Purification for $^{100}Sn(60MeV/u)$ with charge states

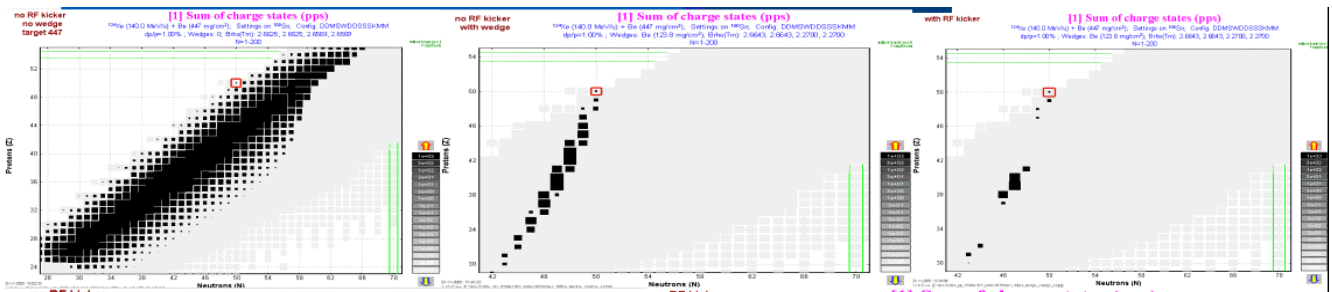

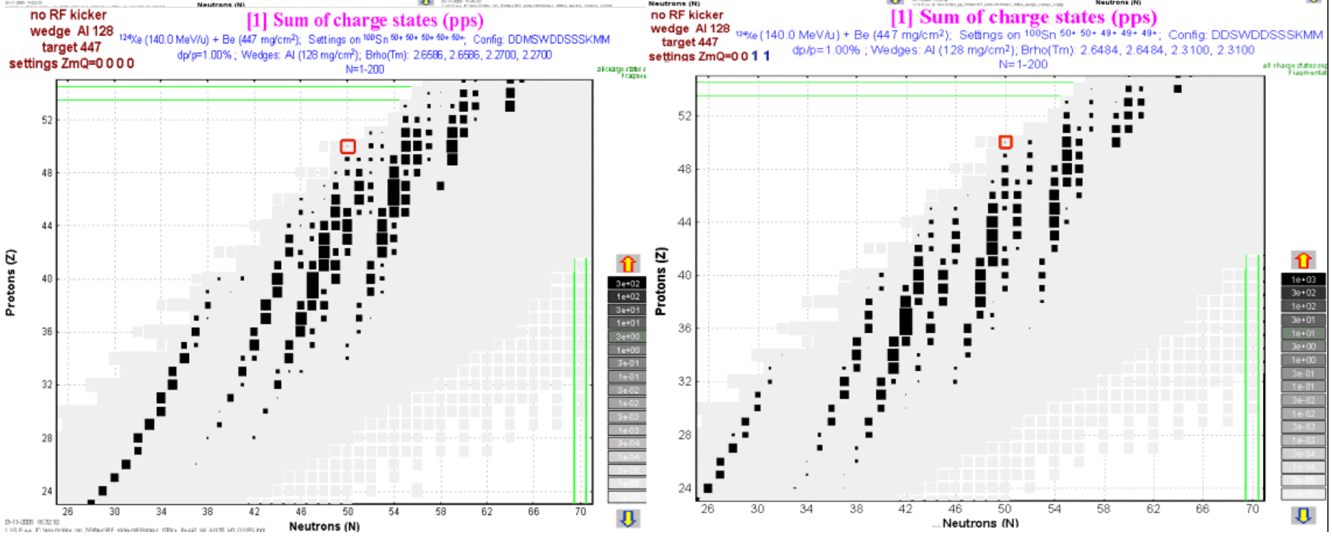

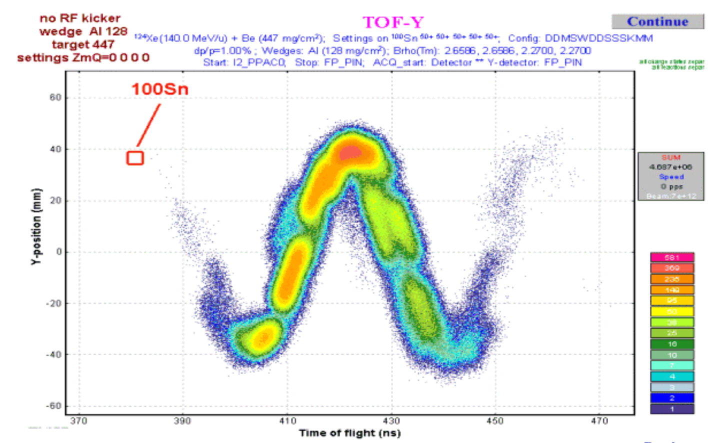

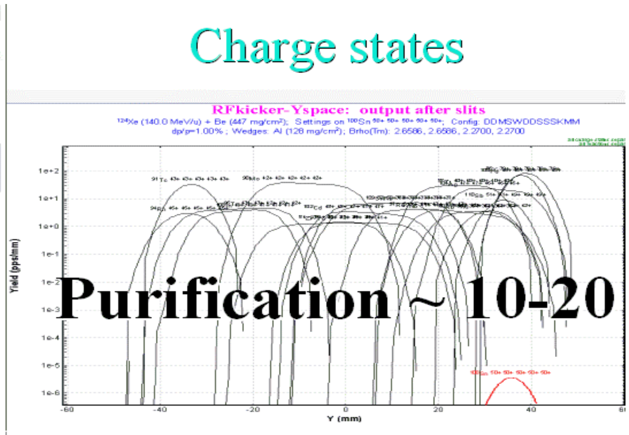

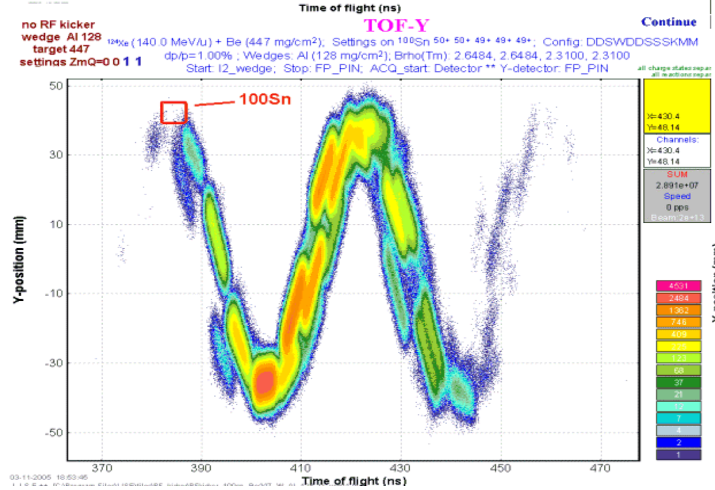

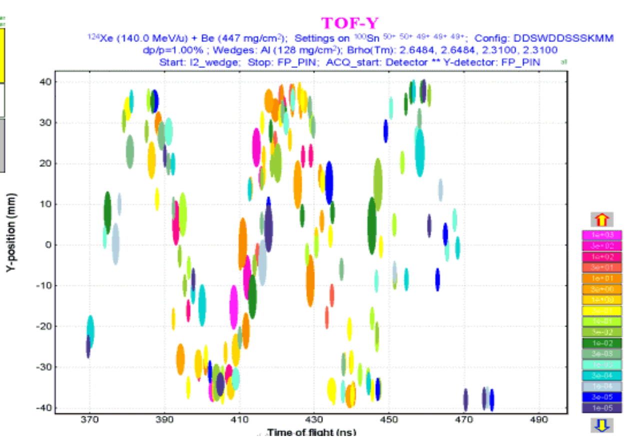

Purification ~ 1 000

1.6.4. Low frequency

It is possible also to solve this problem with:
* Increase the fragment energy
* Decrease the length of flight

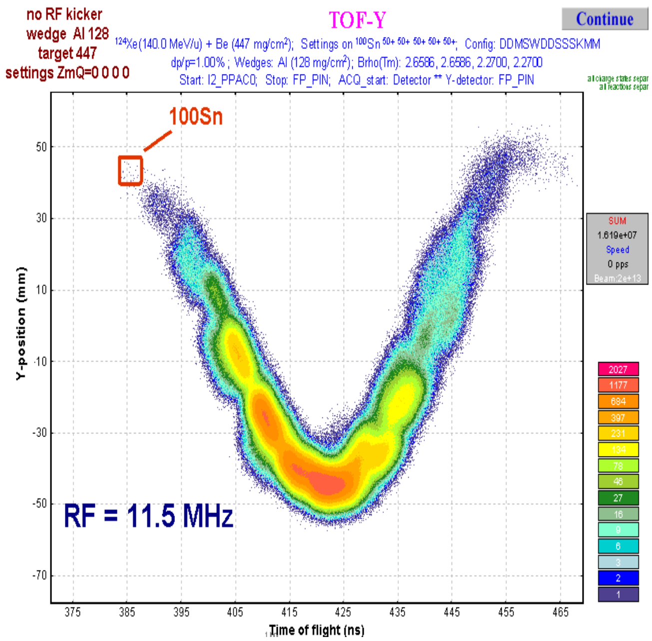

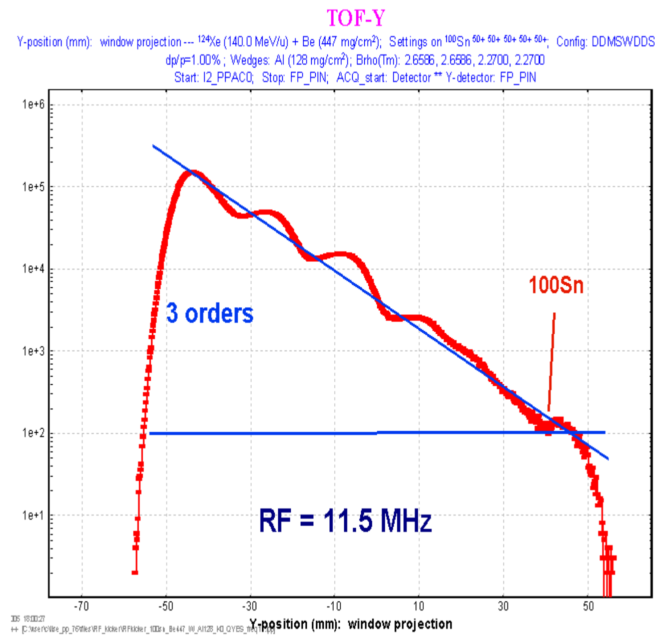

1.6.5. Short flight base (35 m)

Purification ~ 90

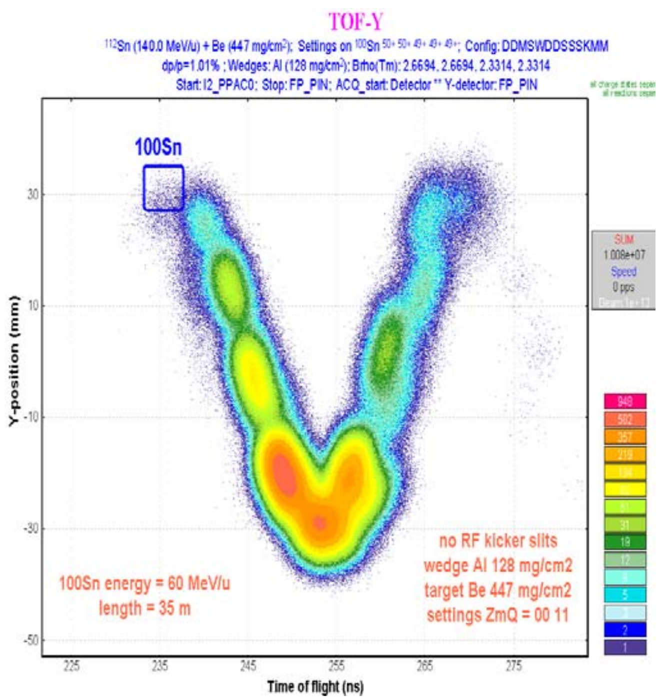

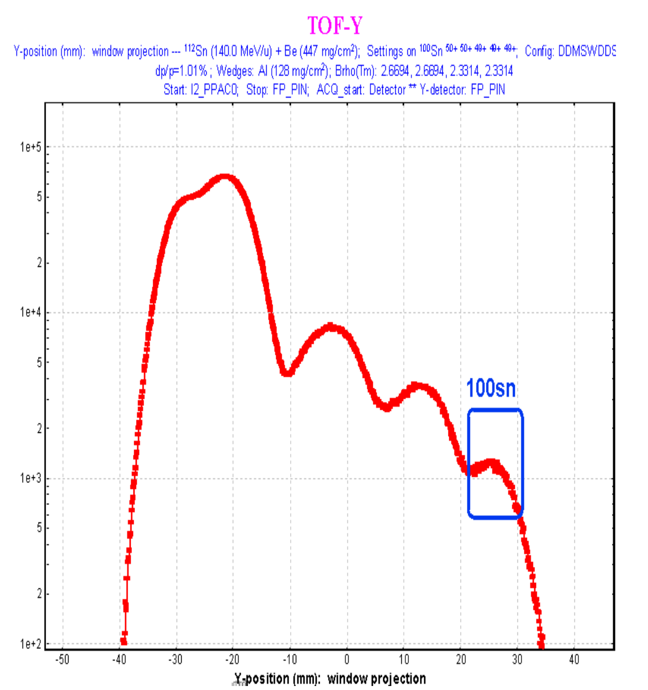

1.6.6. High energy (105 MeV/u)

Purification ~ 120

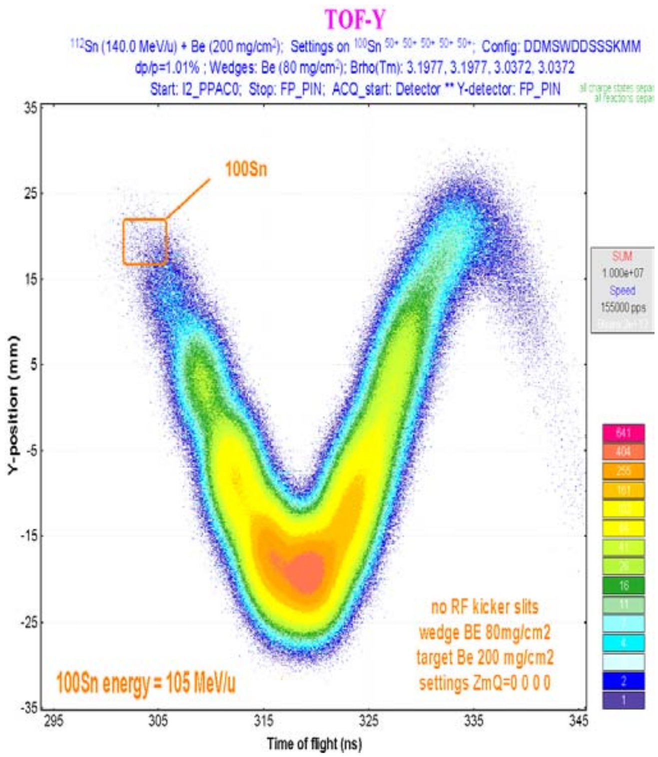

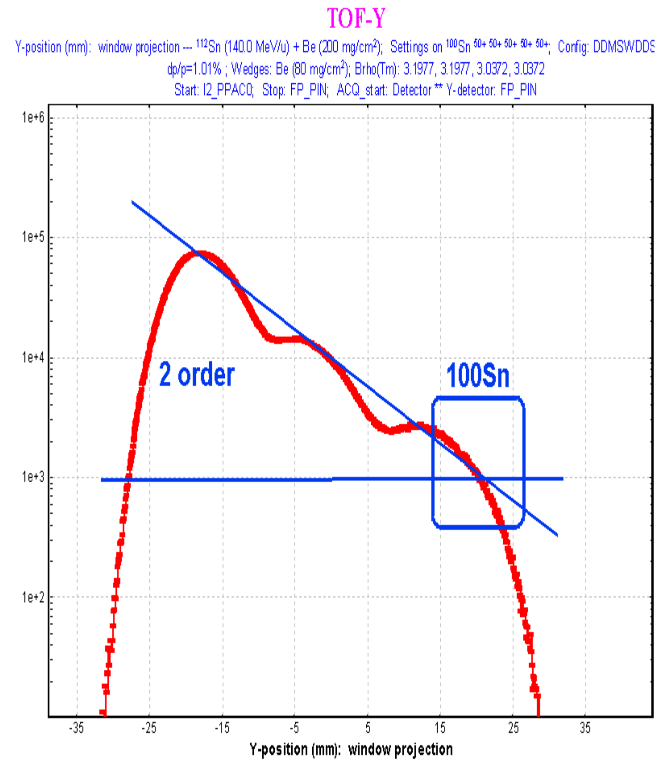

1.6.7. Short flight base (35 m), High energy (105 MeV/u)

Purification ~ 300

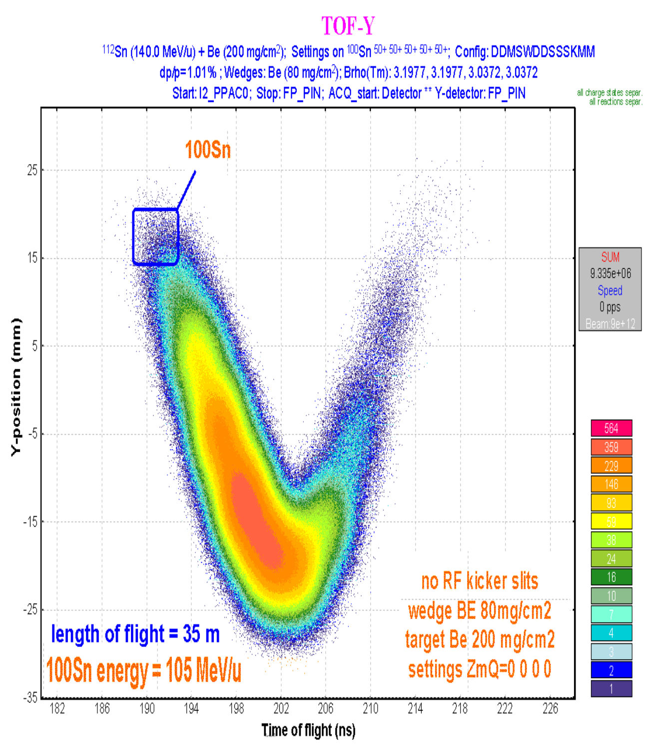

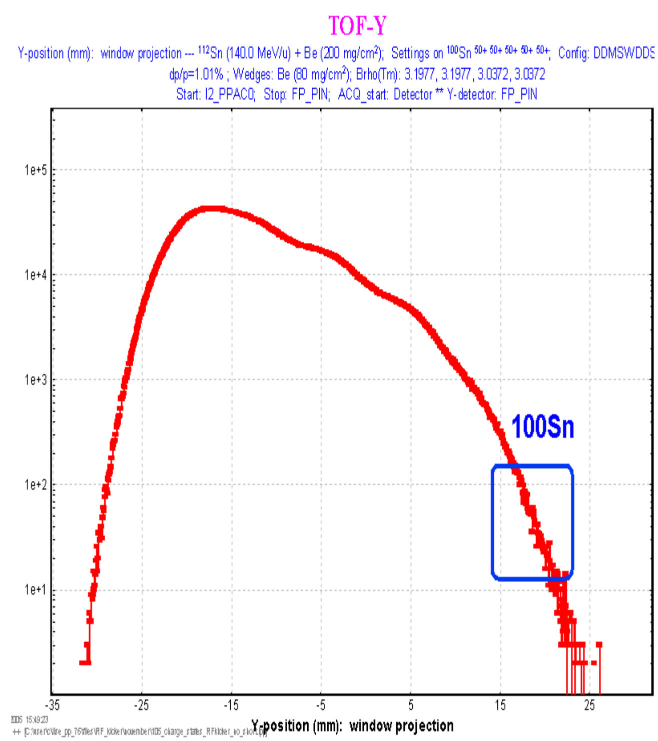

Acknowledgements

The LISE++ authors thank Dr. Marc Doleans for help in developing the RF kicker block in the code.

References:

[RFS05] RF kicker proposal, V. Andreev, D.Bazin, M. Doleans, D.Gorelov, F. Marti, X. Wu; "RF-KICKER SYSTEM FOR SECONDARY BEAMS AT THE NSCL", D. Gorelov, V. Andreev, D. Bazin, M. Doleans, T. Grimm, F. Marti, J. Vincent, X. Wu, Proceedings of 2005 Particle Accelerator Conference, Knoxville, Tennessee; http://accelconf.web.cern.ch/accelconf/p05/PAPERS/FPAE072.PDF.

[Yam04] K.Yamada et al., Nuclear Physics **A746** (2004) 156c-160c.